*Laser Chem.*, 2002, Vol. 20(1), pp. 23–32

Taylor & Francis
Taylor & Francis Group

# LASER ABLATION STUDIES OF DEPOSITED SILVER COLLOIDS ACTIVE IN SERS

R. TORRES LA PORTE[a], D. SILVA MORENO[a], M. CASTILLEJO STRIANO[a], M. MARTÍN MUÑOZ[a]* J. V. GARCÍA-RAMOS[b], S. SÁNCHEZ CORTÉS[b] and E. KOUDOUMAS[c]

[a]*Instituto de Química Física "Rocasolano", C.S.I.C., Serrano 119, 28006 Madrid, Spain*; [b]*Instituto de Estructura de la Materia, C.S.I.C. Serrano 121, 28006 Madrid, Spain*; [c]*Institute for Electronic Structure and Laser, FORTH, P.O, Box 1527, 711 10 Heraklio, Greece*

*(Received 21 May 2001)*

Laser ablation of deposited silver colloids, active in SERS, is carried out at three different laser wavelengths (KrF, XeCl and Nd:YAG at $\lambda = 248$, 308 and 532 nm respectively). Emission form excited neutral Ag and Na atoms, present in the ablation plume, is detected with spectral and temporal resolution. The expansion velocity of Ag in the plume is estimated in $\sim 1 \times 10^4$ m s$^{-1}$. Low-fluence laser ablation of the colloids yields ionized species that are analyzed by time-of-flight mass spectroscopy. $Na^+$ and $Ag_n{}^+ (n \leq 3)$ are observed. Composition of the mass spectra and widths of the mass peaks are found to be dependent on laser wavelength, suggesting that the dominant ablation mechanisms are different at the different wavelenghts.

*Keywords*: Laser ablation; Silver colloids; SERS active silver surfaces

## 1. INTRODUCTION

Inhomogeneous metal surfaces are known to induce large enhancement of several optical effects. A largely exploited application of this property is Surface-Enhanced Raman Spectroscopy (SERS) [1, 2]. Among the differ-

* Corresponding author. E-mail: mmm@iqfr.csic.es

ent SERS substrates, several silver-based surfaces have been found to exhibit SERS activity. Silver films produced by metal vapor condensation onto cold surfaces have been found to posses or not SERS activity depending on the deposition temperature that affects the fractal character of the rough films [3]. For other widely used substrates such as silver colloidal suspensions and silver island films it has been shown that particle size and shape strongly influence SERS activity [4]. This relation between surface morphology and SERS effectiveness has stimulated research aimed at the development of methods to prepare and characterize new types of substrates [5]. A way to characterize morphological differences in surfaces is based on the fact that the process of laser desorption/ablation of metal atoms from surfaces is rather sensitive to particle size [6, 7]. For instance, laser desorption of silver films, of different thickness and surface morphology, give rise to different abundance and rates of $Ag_n$ clusters [8]. Moreover, desorption/ablation of metals with visible radiation at low fluences proceeds through a non-thermal mechanism in which desorption rates, kinetic energy of the desorbed atoms and the fraction of atoms, dimers and large aggregates produced, are dependent on the laser parameters and structure of the surface [7, 9].

Theoretical [10] and experimental [4] work, carried out by some of us, has been aimed at developing more effective SERS substrates. As part of a systematic study to produce and characterize the latter, in this work we have applied laser desorption and ablation techniques to study surfaces composed of deposited silver colloids.

## 2. EXPERIMENTAL

Silver colloids were prepared by the Lee–Meisel method [11] in the following way: 200 ml of a $10^{-3}$ M solution of $AgNO_3$ in water was brought to the boil. 4 ml of a 1% trisodium citrate solution was then added and boiled again for one hour. Some drops from the colloidal solution were deposited on a polyacetate sheet or on a quartz plate and dried in an oven at 37°C for 3 h.

Low fluence laser ablation of the deposited colloids and time-of-flight mass spectrometric analysis of the ejected species were performed in the following way. Interaction of the laser with the colloidal sample took place inside a vacuum chamber that houses a set of parallel plates to extract and accelerate the ions. The chamber was pumped to $10^{-6}$ Torr. The laser beam, mildly focused, entered the vacuum chamber perpendicularly to the

time-of-flight axis, at normal incidence to the surface of the samples. The latter were placed between the two first plates, at a distance of 3 mm from the axis of the set of parallel plates. A translation/rotation mount allowed displacements of the sample preventing repeated exposure to the laser of the same spot. Typical voltage differences between the first two plates were 200–400 V. The drift region of 1 m long was evacuated to $10^{-7}$ Torr. The ions were detected by a set of microchannel plates and the time-of-flight spectrum was recorded by a digital oscilloscope (Tektronix 2430 or LeCroy 9414) and transferred to a microcomputer.

The mechanism of ablation was also investigated by optical time-of-flight spectroscopy. The laser beam was focused on the sample at normal incidence by a 9 cm focal length lens; the sample was placed inside a vacuum cell provided with quartz windows. Prior to the time resolved measurements, the time integrated emission spectrum originating in the ablation plume was recorded by means of a spectrograph (DKSP-240) coupled to a CCD camera (SBIG, ST-6V). For the optical time-of-flight measurements, the visible plasma of the ablation plume extending $\sim 2$ cm above the sample surface was 1:1 projected onto the entrance slit of a high intensity Bausch and Lomb monochromator (f/3.5, spectral resolution was 0.6 nm, spatial resolution was 100 μm). The sample was translated in steps of 1 mm perpendicularly to the sample surface (parallel to the focal plane of the projecting lens) and could be rotated to avoid repeated exposure of the same spot to the laser light. In order to maintain, throughout the measurements, the same laser focusing conditions on the sample, the lens that focused the laser beam was translated together with the sample. At each position, a different slice of the plume was projected onto the monochromator slit and the dispersed emission detected by a photomultiplier (EMI 9816QB). The time resolved photomultiplier signal was recorded and averaged by an oscilloscope (Tektronix TDS 220, 50Ω loading resistance, 100 MHz).

The fluorescence spectrum, excited by the laser, on the colloids deposited on a quartz plate, was recorded. The unfocused laser beam (KrF at 248 nm) illuminated the sample at an incidence angle of 45°. Laser energies were in the range of 0.5–1 mJ. The fluorescence from the sample was collected at right angles to the laser beam and imaged onto the entrance slit of the monochromator. The photomultiplier signals were fed into a Gated Integrator and Boxcar Averager (SRS 250) connected to a PC through a SRS 245 computer interface.

## 3. RESULTS AND DISCUSSION

### 3.1. Fluorescence Spectra

Ultraviolet laser excitation at 248 and 266 nm of the silver colloids deposited on a quartz plate, gives a fluorescence emission with a single maximum in the region 440–460 nm. The possibility that the substrate or other impurities present in the silver colloids, could add some contribution to this emission was examined. Neither the quartz substrate nor the sodium salt, used in the colloids preparation method, gave emission under similar excitation conditions, giving support to the conclusion that the fluorescence can be attributed to the silver colloidal sample. However, assignment of this emission to previously reported transitions in silver colloids is not straightforward. It has been shown that the absorption spectra of colloids, in aqueous solution, show a band near 400 nm that shifts and splits, as a function of shape and size of the surface particles and surface-adsorbed species [4, 12]. A relation between the fluorescence band from the deposited colloids described here, and the colloidal absorption bands is highly unlikely. The transition near 400 nm, associated with the well known dipolar surface plasmon for silver spherical particles, gives rise to electron excitation that relax by non-radiative channels in the subpicosecond time scale [12, 13]. On the other hand, mass selected small silver clusters trapped in cryogenic matrix, excited at wavelengths near 260 nm, give also fluorescence emission near 450 nm [14]. However, there is no evidence to relate the emission from the deposited colloids studied here with that of small clusters. An improved design of the colloids preparation method to obtain samples free of byproducts, and work involving samples prepared with different degrees of particle aggregation, would be of help in the assignment of the fluorescence observed here.

### 3.2. Optical Time-of-Flight Analysis

In order to get some information about the evolution of the uncharged atomic species in the plume, we have analyzed the emission originating in excited neutral atomic silver, with time and spatial resolution.

The time integrated emission spectrum from the plasma produced by KrF laser ablation of the deposited colloids, gives several lines corresponding to excited states of neutral Ag and Na. At a laser fluence of 1J $cm^{-2}$ the spectrum shows the strong Ag(I) atomic lines at 327 and 338 nm, the less in-

tense at 520 and 546 nm and excited Na(I) emission at 589 nm; the time integrated spectrum does not show any appreciable contribution from continuous background emission. Na(I) is related to the presence of sodium salts resulting in the preparation process of the colloid. Molecular bands corresponding to excited CN and $C_2$ also appear in the spectrum and are characteristic of the polymer substrate on which the samples are deposited. The atomic transition for silver emission at 327 nm and Na at 589 nm are respectively Ag($5p\ ^2P_J{}^0 \rightarrow 5s\ ^2S_{1/2}$) and Na($3p\ ^2P_J{}^0 \rightarrow 3s\ ^2S_{1/2}$). Radiative lifetimes of the excited Ag and Na are 6.7 and 16.4 ns [15]. No emission corresponding to ionized species was observed.

The time resolved emission at distances above the surface in the range of 4 to 8 mm was recorded for the Ag line at 327 nm. The time resolved emission from Na at 589 nm was also recorded at distances from the surface from 2 to 7 mm. The temporal behavior of the emissions at each distance follows qualitatively the evolution described for other plasma emissions. Very near the surface, the atomic emission is hidden by the fast signal that comprises the luminous front of the plasma [16]. At 4 mm above the surface, the fast signal and the excited Ag atomic emission appear temporally resolved; the latter has a maximum near 100 ns and full width at half maximum (FWHM) of about 125 ns. At increasing distances, the intensity of the scattering signal decreases and becomes negligible; the atomic emission broadens and its maximum decreases in intensity and shifts towards longer times. The time of the maximum emission is plotted versus distance to the surface obtaining that its dependence on distance is close to linear. This is depicted in Figure 1. From the reciprocal of the slope, it can be estimated the expansion velocity of excited Ag is $1 \times 10^4$ m $s^{-1}$. The emission from excited Na was analyzed in a similar way and the time of the maximum intensity at each distance is also plot in Figure 1. A similar behavior and expansion velocity is obtained within experimental error.

The above measurements show that formation of excited Ag in the plume expansion holds at a relatively large distance above the surface. On the other hand, the nearly constant slope of the plot representing time versus distance, shown in Figure 1, seems to indicate that a single mechanism is responsible for the formation process, at distances greater than 4 mm. In other systems, where emission from both excited ions and neutrals can be detected, three body ion recombination with low energy electrons has been postulated to play a role in the formation of excited states of atoms at distances of the surface larger than 2 mm [17, 18]. Although more accu-

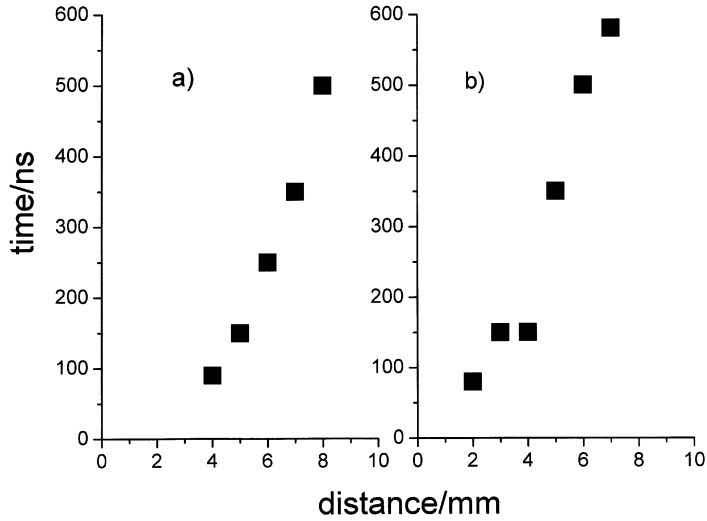


FIGURE 1 Delay between laser pulse and maximum of the emission recorded at different distances above the surface. a) Emission from excited Ag(I) at 327 nm. b) Emission from excited Na(I) at 589 nm.

rate data would be needed in order to clarify the nature of the participating processes, we tentatively conclude that, in the present system, ion recombination is a plausible mechanism and therefore excited Ag formation could be related to $Ag^+$ ion expansion within the plume.

### 3.3. Time-of-Flight Mass Spectrometric Analysis

The mass spectra obtained in the laser desorption/ablation of the colloidal samples were recorded at three different laser wavelengths, KrF laser at 248 nm, XeCl at 308 nm and the second harmonic of the Nd:YAG at 532 nm. In the three cases the laser energy and fluence were kept to the minimum value above the threshold for signal observation; typical values were in the range of 200–340 μJ, with estimated fluences of 50–100 mJ $cm^{-2}$. Single laser shot spectrum was recorded and several stored spectra were averaged. Values for m/z were obtained by fitting the time-of-flight spectrum to a second order polynomial, $m/z = a.t^2 + b.t + c$

Figure 2 depicts the mass spectra obtained at the three laser wavelengths. At 248 nm the observed peaks can be assigned to $Na^+$, $Ag^+$ and $Ag_2{}^+$. The same three peaks appear under laser ablation at 308 nm, together with two

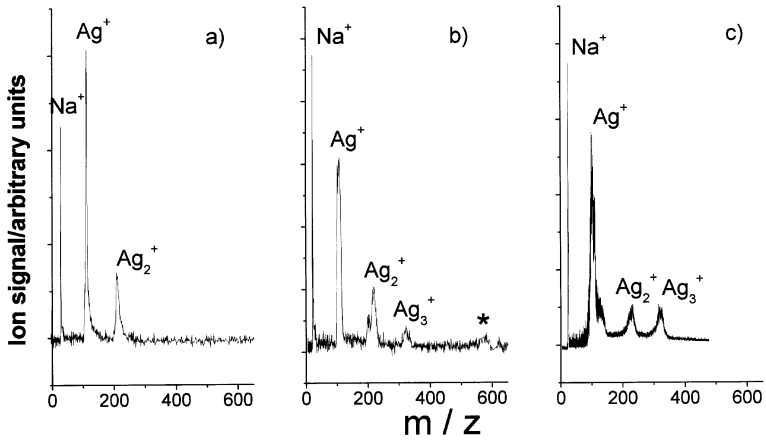


FIGURE 2 Time-of-flight mass spectra obtained in the laser ablation of deposited silver colloids, at different laser wavelengths. a) KrF laser at 248 nm. b) XeCl at 308 nm. c) Nd:YAG at 532 nm.

more peaks. The peak at shorter time can be readily assigned to $Ag_3^+$ whereas for the peak at longer times the assignment is uncertain although it is close to the m/z value corresponding to a five atom silver cluster. At 532 nm the spectrum is similar to that obtained at 308 nm with the exception of the highest mass peak that is not observed. As stated above, $Na^+$ is related to the presence of Na salts formed as a result of the colloids preparation method. The relatively broad peaks do not allow resolution of the silver isotopes. For the three wavelengths the narrower peak is $Na^+$. At similar laser powers, the mass spectrum obtained upon laser ablation at 248 nm leads to a narrower peaks than at the longer wavelengths. A simple calculation, modeling the fields and geometry of the time-of-flight apparatus, shows that the main factor influencing the spectral widths is the velocity distribution in the direction perpendicular to the accelerating field, therefore indicating that $Ag^+$ and $Ag_n^+$ are formed with a hot velocity distribution.

Regarding the ion velocity, in the direction perpendicular to the sample surface, preliminary measurements have been carried out in a time-of-flight mass spectrometer of a different configuration; in this, the sample is placed perpendicular to the time-of-flight axis and pulsed extracting fields can be applied. Measuring the delay between laser firing and the bias voltage pulse that optimizes ion signal intensity, it is possible to estimate the $Ag^+$ velocity in the direction perpendicular to the sample surface as

$\sim (0.2–0.4) \times 10^4$ m $s^{-1}$. This velocity, obtained for ablation at the laser wavelength of 532 nm, can be compared to the larger value of $1 \times 10^4$ m $s^{-1}$ estimated for excited Ag neutrals (section 3.2) measured upon KrF laser ablation of the samples.

Measurements of the kinetic energy distributions for the $Ag_n$ cations and neutrals, generated in the laser desorption/ablation of metal surfaces of different morphologies, at different ultraviolet and visible laser wavelengths, indicate that, at low laser fluences, a non-thermal process occurs; large kinetic energy values and narrow velocity distributions are obtained in all cases. The kinetic energy distribution does not show a wavelength dependence [9, 20], but it has been found that, as the laser fluence grows, a gradual transition to thermal evaporation takes place [9]. Mean velocity and width of the distributions are different for the different surfaces [7–9, 20] and can be dependent on characteristics of the surface such as total coverage of metal atoms on the substrate and surface defects [9]. We conclude that detailed work, aimed at obtaining the kinetic energy distribution of the ions formed under the different laser wavelengths, is needed in order to better characterize the colloidal system studied here; this information would also help to elucidate the relation between the evolution of neutrals and ions within the ablation plume.

A final point to be considered is the differences in mass composition obtained in this work, depending on wavelength of the ablating laser. At $\lambda = 532$ nm and fluences in the same range as those of the present work, laser desorption studies of thin silver films indicate that the mechanism of electronic excitation desorption, yield monomer silver cations and neutral clusters but no $Ag_n^+$ clusters; the latter are assumed to be formed as the result of reactions within the ablation plume [8]. However, also for metal surfaces of different morphologies, changes of the mass composition of the desorbed species with exciting laser wavelength, have been attributed either to differences in the excitation mechanism within the solid [20] or correlated to the conditions in which transition from non-thermal desorption to thermal evaporation take place [9]. In this latter case, some evidence indicates that the heavier species are directly desorbed from the surface rather than formed by gas phase collisions. A tentative conclusion is that the changes in mass composition with ablation wavelength, reported here, might reflect the participation, at the longer wavelengths, of a thermal ablation mechanism. This would also be consistent with the larger widths of the peaks in the mass spectra obtained at the longer laser wavelengths.

However, we note that at a given wavelength laser fluence marks the transition from the non-thermal to the thermal regime. Therefore, the present results do not exclude the participation, at the longer wavelengths, of a non-thermal process, providing that ablation were carried out at a fluence closer to the ablation threshold.

## 4. FINAL SUMMARY AND REMARKS

Laser ablation/desorption of deposited silver colloids, at three different wavelengths has been studied. Analysis of the ablation plume shows the presence of excited neutral and ionized Ag atoms and $Ag_n^+$ cluster ions. The mass composition of the ablation plume has been measured and the expansion velocity of neutral and ionized Ag have been estimated at different laser wavelengths. At 248 nm, larger velocities (assuming that the formation mechanisms in the plume for excited Ag is related to $Ag^+$) and narrower distributions (narrower time-of-flight spectral peaks) are estimated as compared to those found at the 308 and 532 nm laser wavelengths. The mass composition is also different at the different wavelenghts; ablation at 308 and 532 nm shows the presence of the heavier cluster $Ag_3$, absent at 248 nm. The results seem to indicate that different ablation mechanisms operate at the different wavelengths. Comparison with results obtained for other metal substrates suggests that, at 308 and 532 nm, at the fluences used for the experiments, thermal processes have a large contribution to the desorption mechanism.

### *Acknowledgments*

Financial support has been provided by Spanish DGI, MCyT (BQU2000-1163-CO2-01) and by the Ultraviolet Laser Facility operating at FORTH-IESL under the EU contract HPRI-1999-CT-00074. Thanks are also given to M. Velegrakis for performing the velocity measurements on the silver monomer ion.

### *References*

[1] Moskovits, M. (1985). *Rev. Mod. Phys.*, **57**, 783.
[2] Campion, A. and Kambhampati, P. (1998). *Chem. Soc. Rev.*, **27**, 241.

[3] Douketis, C., Wang, Z., Haslett, T. L. and Moskovits, M. (1995). *Phys. Rev. B.*, **51**, 11022.
[4] Rivas, L., Sánchez-Cortés, S., García-Ramos, J. V. and Morcillo, G. (2001). *Langmuir*, **17**, 574.
[5] Mafuné, F., Kohno, J-Y., Takeda, Y. and Kondow, T. (2000). *J. Phys. Chem. B.*, **104**, 9111.
[6] Vollmer, M., Weidenauer, R., Hoheiesel, W., Schulte, U. and Träger, F. (1989). *Phys. Rev. B.*, **40**, 12509.
[7] Hoheisel, W., Vollmer, M. and Träger, F. (1993). *Phys. Rev. B.*, **48**, 17463.
[8] Owega, S., Lai, E. P. C. and Mullett, W. M. (1998). *J. Photoch. Photob. A: Chem.*, **119**, 123.
[9] Götz, T., Bergt, M., Hoheisel, W., Träger, F. and Stuke, M. (1996). *Appl. Surf. Sci.*, **96–98**, 280.
[10] Sánchez-Gil, J. A. and García-Ramos, J. V. (1997). *J. Chem. Phys.*, **108**, 317.
[11] P. C. Lee, and D. Meisel, *J. Phys. Chem.*, **86**, 3391 (1982).
[12] Kamat, P. V., Flumiani, M. and Hartland, G. (1998). *J. Phys. Chem.*, **102**, 3123.
[13] Ahmadi, T. S., Logunov, L. and El-Sayed, M. A. (1996). *J. Phys. Chem.*, **100**, 8053.
[14] Félix, C., Sieber, C., Harbich, W., Buttet, J., Rabin, I., Schulze, W. and Ertl, G. (1999). *Chem. Phys. Lett.*, **313**, 105.
[15] Radzig, A. A. and Smirnov, B. M. (1985). *Reference Data on Atoms*, *Molecules*, *and Ions*. J. P. Toennies (Ed). Springer Series in Chemical Physics **31**, 230.
[16] Green, J. M., Silfvast, W. T. and Wood II, O. R. (1977). *J. Chem. Phys.*, **48**, 2753.
[17] Marine, W., Scotto d'Aniello, J. M., Gerri, M. and Thomsen-Schmidt, P. (1992). In: *Laser Ablation of Electronic Materials*. Fogarassy, E. and Lazare, S. (Ed). Elsevier Sci. Publ. B.V. p. 89.
[18] Gonzalo, J., Ballesteros, J. M. and Afonso, C. N. (1999) *Appl. Surf. Sci.*, **138–139**, 52.
[19] Owega, S., Lai, E. P. C. and Bawagan, A. D. O. (1998). *Anal. Chem.*, **70**, 2360.
[20] Helvajian, H. and Welle, R. (1989). *J. Chem. Phys.*, **91**, 2616.